# Structural Change of $Li_{1-x}Ni_{0.5}Mn_{0.5}O_2$ Cathode Materials for Lithium-ion Batteries by Synchrotron Radiation

Yoshinori Arachi,* Hironori Kobayashi,† Shuichi Emura,†† Yoshiyuki Nakata,††† Minoru Tanaka, and Takeshi Asai
*Unit of Chemistry, Faculty of Engineering, Kansai University, Suita, Osaka 564-8680*
†*National Institute of Advanced Industrial Science and Technology (AIST), Ikeda, Osaka 563-8577*
††*ISIR, Osaka University, Ibaraki, Osaka 567-0047*
†††*Faculty of Science and Engineering, Iwakimeisei University, Iwaki, Fukushima 970-8551*

(Received September 24, 2002; CL-020816)

Synchrotron X-ray diffraction and XAFS measurement have been employed to investigate structural change and the charging process of a layered $LiNi_{0.5}Mn_{0.5}O_2$ cathode material. The structure of charged $Li_{1-x}Ni_{0.5}Mn_{0.5}O_2$ ($x = 0.5$), which corresponds to the composition for showing rechargeable capacity, was determined. The results showed that divalent nickel metal was oxidized to trivalent after charging, in association with the phase transition from hexagonal ($R\bar{3}m$) to monoclinic ($C2/m$) resulting from the ordering of cations in the layered structure.

In view of small natural deposits of Co and its toxicity, new cathode materials that can serve as alternatives to $LiCoO_2$ in lithium ion batteries, such as $LiNiO_2$ or $LiMn_2O_4$, have been extensively pursued. Several problems, including thermal stability and capacity fading at elevated temperature, limit practical utilization, and few materials satisfy all properties that support high performance. Recently, Ohzuku et al. have proposed $LiNi_{0.5}Mn_{0.5}O_2$ as a new cathode material for rechargeable lithium batteries.[1] Cell performance using Li exhibited good cycleability, and a reversible capacity of 150 mA h/g within the voltage range of 3.0 to 4.3 V, which corresponds to one-half of theoretical capacity (280 mA h/g). However, the details of the crystal structure of $LiNi_{0.5}Mn_{0.5}O_2$ and the mechanism of charging process remain unclear. Dahn et al. reported $Li[Ni_xLi_{(1/3-2x/3)}Mn_{(2/3-x/3)}]O_2$ with $x = 1/3$, 5/12, 1/2, which showed a capacity of 200, 180, 160 mA/g, respectively between 2.0 and 4.6 V.[2] They described that $Ni^{2+}$ and $Mn^{4+}$ coexist in the layered materials. When Li is deintercalated from the material, $Ni^{2+}$ is oxidized to $Ni^{4+}$, while $Mn^{4+}$ retains its oxidation state. We adopted this fascinating material in order to investigate the structural change and deintercalation behavior during charging process by the diffraction technique, in addition to the local structural change by XAFS. In this study we focused on the composition of $x = 0.5$ in $Li_{1-x}Ni_{0.5}Mn_{0.5}O_2$, which determines the reversible capacity.

Samples were prepared from $LiOH{\cdot}H_2O$ and dry precipitates of $Ni(OH)_2$ and $Mn(OH)_2$ which were kindly supplied by TOSOH Company. They were mixed and then calcinated at 600 °C for 12 h. The obtained powders were pressed into a disk under a pressure of 5 t/cm$^2$, and sintered at 1000 °C for 12 h. Lithium was electrochemically deintercalated at a rate of 170 µA/cm$^2$, by use of a coin-type cell. The cathode material was composed of the following materials; sample: acetylene black: poly vinylidene fluoride (PVDF) = 86 : 4 : 10 in wt%, and 1 M $LiClO_4$ in propylene carbonate(PC) : 1,2-dimethoxycarbonate(DMC) = 1 : 1 by volume was used as the electrolyte. X-ray diffraction measurement was performed by use of synchrotron radiation, at a wavelength of $\lambda = 0.500$ Å on BL02B2 at SPring-8. Rietveld crystal structural refinement was carried out by use of the program RIETAN-2000.[3] X-ray absorption measurements at the Mn- and Ni-K edges by transmission mode were performed on BL01B1 at SPring-8. The in situ cell was assembled at the globe box. The software programs WinXAS2.1[4] and FEFF8.10[5] were used for XAFS analysis. These synchrotron radiation experiments were performed at the SPring-8 with the approval of the Japan Synchrotron Radiation Research Institute (JASRI) (Proposal 2001B0484-NX-np, 2002A0370-ND1-np).

Figure 1 shows the XRD patterns for lithium-deintercalated samples. All the peaks for $x = 0.0$, 0.1, 0.2 were indexed with hexagonal lattice, and the results confirm the formation of a single phase related to the layered structure, such as $LiCoO_2$, $R\bar{3}m$ lattice. Each sample corresponds to the composition in the charge and discharges curves as shown in Figure 2. The Rietveld refinement analysis was based on conventional layered rock salt type structure. Rietveld refinement yielded agreement factors $R_{wp} = 3.50$, $R_p = 2.36$, and $R_I = 1.73$, with expected agreement $R_e = 1.36$ for $x = 0.0$ ($a = b = 2.8910\underline{9}$ Å, $c = 14.29\underline{7}$ Å). The ion distribution indicates that a small amount of Ni (occupancy, $g = 0.09\underline{3}$) occupies the Li (3$b$) site. Neutron diffraction supported this result well. $Ni^{2+}$ is located at both the 3$a$ and 3$b$ sites, whereas $Mn^{4+}$ is located only at the 3$a$ site. The details will be described elsewhere. In contrast, the XRD patterns for $x = 0.3$, 0.4, 0.5 show mainly monoclinic lattice, in addition to a small amount of the host phase. This result was confirmed by the

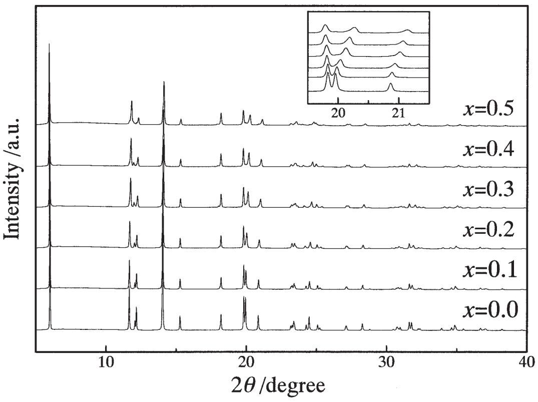

**Figure 1.** X-ray diffraction patterns for $Li_{1-x}Ni_{0.5}Mn_{0.5}O_2$. Lithium was electrochemically deintercalated at a rate of 170 µA/cm$^2$ using coin-type cell. The insert is shown in the expansion of characteristic peaks.

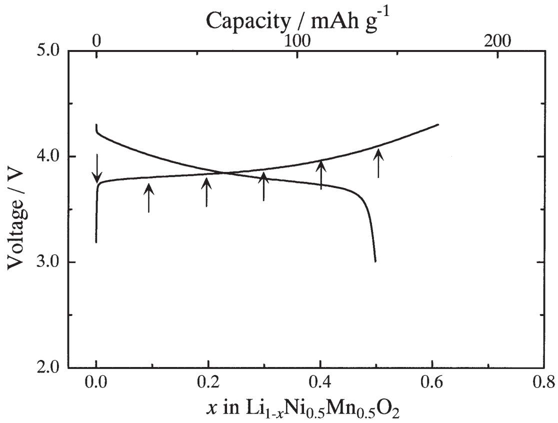

**Figure 2.** Charge and Discharge curves of the Li/ $Li_{1-x}Ni_{0.5}Mn_{0.5}O_2$ cell measured with a current density of 0.1 mA/cm$^2$ and cut-off voltages of 3.0 and 4.3 V. The arrows show the composition used in XRD and XAFS measurements.

observation of electron diffraction patterns by high resolution-TEM as well. The structure for $x = 0.5$ was refined with the monoclinic lattice ($C2/m$; $a = 4.924\underline{2}$ Å, $b = 2.852\underline{3}$ Å, $c = 5.087\underline{5}$ Å, $\beta = 108.81\underline{5}°$). The change of lattice parameter during the charging process is summarized as follows: $a$ and $b$ in the plane of the structure decrease linearly, and $c$ of the vertical axis increases. The charging process corresponds to electrochemical Li extraction from the layered structure of $Li_{1-x}Ni_{0.5}Mn_{0.5}O_2$, associated with the oxidation reaction of transition metals (Ni or Mn). The change in lattice parameters can be explained by decreased ionic radius of oxidized transition metals and electrostatic repulsive force between oxygen ions, after lithium is extracted. Figure 3 shows the representative XANES spectra for charged $Li_{1-x}Ni_{0.5}Mn_{0.5}O_2$ by use of an in situ cell. As the cell charged, the XANES spectra of Ni-K edge showed a chemical shift towards higher energy within the voltage range of 3.0–4.1 V. Divalent nickel and tetravalent manganese are located at the octahedral site. This was identified by comparing these spectra with NiO, $LiNiO_2$ and $Li_2MnO_3$. The oxidation of $Ni^{2+}$ occurred after charging, whereas no chemical shifts were observed in the Mn-K edge. The extraction of Li was found to proceed in association with oxidation of $Ni^{2+}$ to $Ni^{3+}$, not oxidation of Mn.

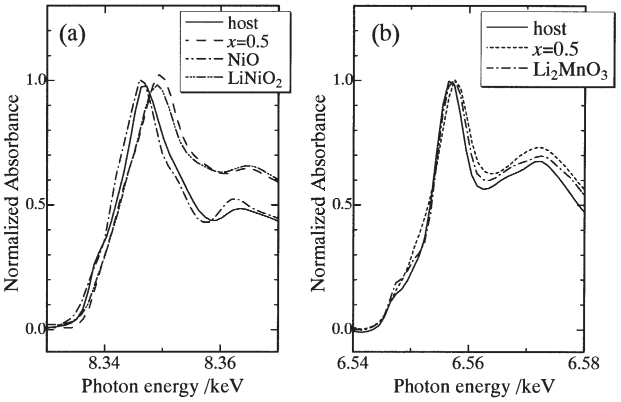

**Figure 3.** XANES spectra of (a) Ni- and (b) Mn-K edge for $Li_{1-x}Ni_{0.5}Mn_{0.5}O_2$ and each standard compounds. The sample was charged at a rate of 200 µA/cm$^2$. The electrolyte was 1 M $LiBF_4$ in ethylene carbonate(EC) : diethyl carbonate(DEC) = 1 : 1 by volume.

Figure 4 shows the Fourier transforms of (a) Ni- and (b) Mn-K edge for $Li_{1-x}Ni_{0.5}Mn_{0.5}O_2$ after the charging process. The spectra in both figures show similar features in relation to the radial distribution, in reflection of the two metals being placed in the same environment. In Figure 4(a), the first peak in the FT corresponds to the nearest neighbors (N.N.) of Ni; i.e., an Ni–O shell in the structure. The second peak in the FT corresponds to the next nearest neighbors (N.N.N.) of Ni; i.e., an Ni-Cation shell where the cation can be either Ni or Mn. The first peak was shifted to shorter distance after charging, since the oxidation of $Ni^{2+}$ to $Ni^{3+}$ shortens the bonding length of Ni–O. Meanwhile, no shift was observed in the Mn-K edge, as shown in the Figure. By use of the structural model obtained by the X-ray diffraction analysis, the backscattering amplitude and phase parameter were calculated by FEFF and fitting was carried out. The results showed that as the cell charged, the distance of the first neighbor Ni–O decreased as a result of reduction in the ionic radius of nickel. A structure model using two shells yielded good fitting for the composition of $x = 0.5$ ($R = 2.49\%$), because Ni and O in monoclinic phase showed two different bonding distances ($2.05\underline{3}$ Å for host, $1.91\underline{5}$ Å (C.N. = 4.0) and $2.04\underline{3}$ Å (C.N. = 2.0) for $x = 0.5$). The details will be reported in the near future.

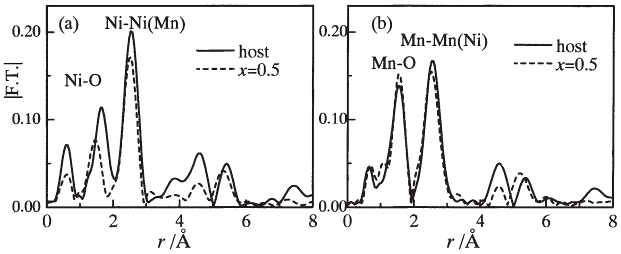

**Figure 4.** Fourier transforms of (a) Ni- and (b) Mn-K edge EXAFS for $Li_{1-x}Ni_{0.5}Mn_{0.5}O_2$.

In summary, for $Li_{1-x}Ni_{0.5}Mn_{0.5}O_2$ the structural change and charging process were determined by X-ray diffraction and XAFS measurement. The composition of $x = 0.0$ is a hexagonal lattice in which a small part of Ni occupies the Li(3$b$) site, and as the cell charged the monoclinic phase appeared from the composition of $x = 0.3$. Lithium was removed by the oxidation of Ni, resulting in the ordering of cations in the layer; that is, appearance of the monoclinic phase.

The authors are grateful to TOSOH Company for providing the sample powders used in this research.

## References

1 T. Ohzuku and Y. Makimura, *Chem. Lett.*, **2001**, 744.
2 Z. Lu, D. D. MacNeil, and J. R. Dahn, *Electrochem. Solid-State Lett.*, **4**, A191 (2001).
3 F. Izumi and T. Ikeda, *Mater. Sci. Forum*, **321–324**, 198 (2000).
4 T. Ressler, *J. Phys. IV*, **7**, C2-269 (1997).
5 J. J. Rehr and R. C. Albers, *Rev. Mod. Phys.*, **72**, 621 (2000).